

Supplemental Figure 1. ARF8 and BPEp proteins interact *in vivo* and co-localize in the nucleus.

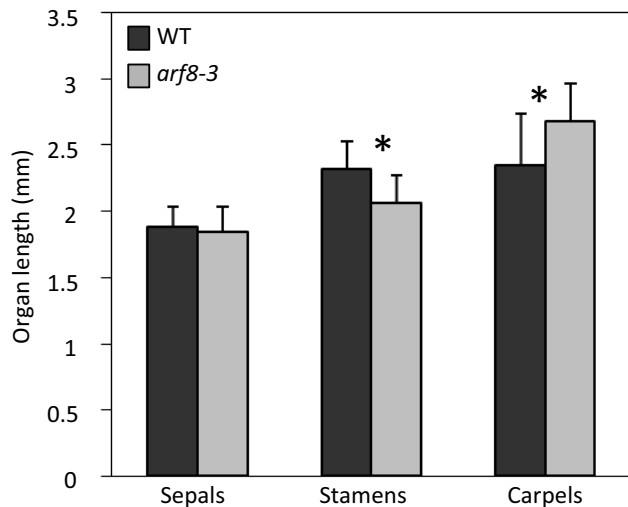
(A-E) ARF8 and BPEp proteins interact *in vivo*. Bimolecular fluorescence complementation (BiFC) assay reveals that the C-terminal domains of BPEp (SD^{BPEp}) and ARF8 (CTD^{ARF8}) interact in tobacco leaf cells. SD^{BPEp} fused to the N-terminal domain of the YFP and CTD^{ARF8} fused to the C-terminal of the YFP were transiently expressed in *Nicotiana benthamiana* leaf cells. Four days post-infiltration, tobacco leaf cells were analyzed on an Axiovert100M LSM-510 laser-scanning Zeiss confocal microscope. SD^{BPEp} and CTD^{ARF8} interact in the cytoplasm of tobacco leaf cells (A). Note that because SD^{BPEp} and CTD^{ARF8} lack the nuclear localization signals of BPEp and ARF8, a cytoplasmic interaction is observed in tobacco cells. SD^{BPEp} mutants R250A (B), D253A (C), F260A (D) and R250A/S251A/D253A (E) lost their ability to interact with ARF8, thus in agreement with the yeast data. For each panel, a fluorescent image (top) and a transmission image (bottom) is presented. Scale bars: 50 μ m.

(F-H) ARF8 and BPEp co-localize in the nucleus of the tobacco cells. BPEp-GFP and mOrange-ARF8 fusion proteins were transiently expressed in *Nicotiana benthamiana* as above, and their cellular localization was analyzed using confocal microscopy. (F) Transient expression of mOrange-ARF8 fusion protein. (G) Transient expression of BPEp-GFP fusion protein. (H) Overlay of (F) and (G) images showing the co-localization of mOrange-ARF8 and BPEp-GFP fusion proteins in the nucleus. Scale bars: 20 μ m.

YVKVSMGDGAPYLRKIDDLKMYKNYPELLKALENMF	IAA1
YVKVSMGDGAPYLRKIDDLKTYKNYPELLKALENMF	IAA2
YVKVSMGDGAPYLRKIDLSCYKGYSELLKALEVMF	IAA3
YVKVSMGDGAPYLRKIDLTMYKQYPELMKSLENMF	IAA4
YVKVSDGAAFLRKIDLEMYKCYQDLASALQILF	IAA5
YMKVSMGDGAPYLRKIDLCIHKGYLELALALEKLF	IAA6
FVKVSMGDGAPYLRKVDLRSYTNYGELSSALEKMF	IAA9
YVKVSMGDGVPYLRKMDLGSSQYDDLAFALEKLF	IAA19
FVKVSMGDGAPYLRKIDDLRMYKSYDELSNALSNMF	IAA17
YVKVSMEGAPYLRKIDDLKTYKSYDELSNALSNMF	IAA27
LVKVSMGDGAPYLRKVDLKMYKSYQDLSDALAKMF	IAA7
FVKVSMGDGAPYLRKVDLRTTYTSYQQLSSALEKMF	IAA8
KQYMFSLRYSGRSLDVYAVRSEKHCNKRS DLCF ²⁷¹	SD^{BPEP}
FVKVYK-SGSVGRSLDI SRFSSYHELREELGKMF	ARF8
FVKVYK-SGSFGRSLDI SKFSSYHELRSELARMF	ARF6
HCKVFMESEDVGRTLDDL SVIGSYQELYRKLAEMF	ARF10
HCKVFMESDDVGRTLDDL SVLGSYEELSRKLSDMF	ARF16
CTKVHKQGIALGRSVDSLKFQNEYELVAELDRLF	ARF2
YTKVQKTGS-VGRSIDVTSFKDYEELKSAIECMF	ARF5
YTKVQKRGS-VGRSIDVNRYRCGYDELRHDLARMF	ARF7
YTKVQKRG-SVGRSIDVTRYSGYDELRHDLARMF	ARF19
CTKVHMQGSAVGRAIDLTRSECYEDLFKKLEEMF	ARF1
CTKVHKQGSQVGRAIDL SRLNGYDDLLMELERLF	ARF4
RTKVQMCGVPVGRAVDLNAIKGYNELIDDI EKLF	ARF9
RIKVQMCGTAVGRAVDLTLIISYDELIKELEKMF	ARF11
RTKVQMCGIAVGRAVDLTLIISYDELIDELEEMF	ARF18
CTKVQMCGVTI GRAVDSL SVLNGYDQLILEEKLF	ARF12
CTKVQMCGVTI GRAVDSL SVLNGYDQLILEEKLF	ARF14
CTKVQMCGVTI GRAVDSL SVLNGYDQLILEEKLF	ARF15
CTKVQMCGVTI GRAVDSL SVLNGYDQLILEEKLF	ARF20
CTKVQMCGVTI GRAVDSL SVLNGYDQLILEEKLF	ARF21
CTKVQMCGVTI ERAVDSL SVLNGYDQLILEEELF	ARF22

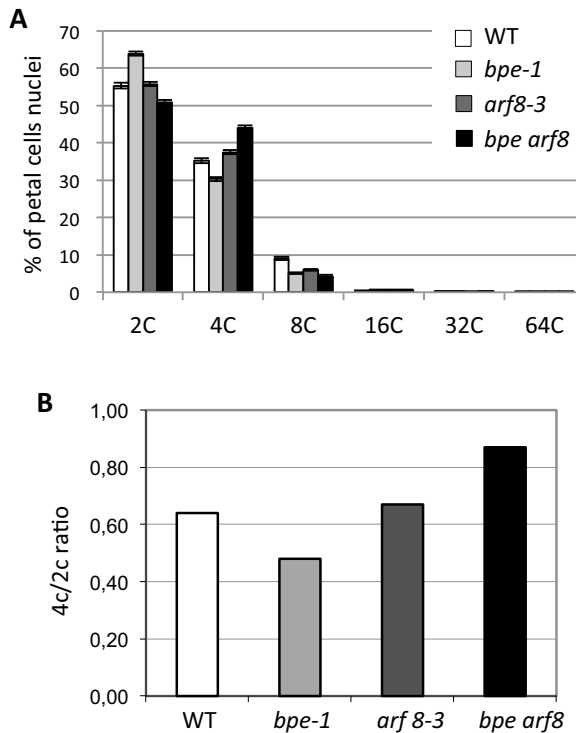
Supplemental Figure 2. Alignment of motif III of ARF and Aux/IAA C-terminal domains with the GRSLD motif of SD^{BPEP}.

Conserved amino acids of the GRSLD motif are highlighted in black background. In grey background are marked amino acids showing high similarity.



Supplemental Figure 3. Sepal, stamen and carpel size in *arf8-3* and wild-type plants.

Sepal, stamen and carpel organ length measurements performed using flowers at development stage 14. Values are given as mean \pm standard error. For each value measurements were performed using at least 60 organs from at least 8 young plants (mutants and wild-type with no mature siliques) of the same age and grown under the same conditions. Asterisks indicate significant differences between wild-type and *arf8-3* with P value < 0.001 (t-test).



Supplemental Figure 4. DNA content of petal cell nuclei.

Nuclei were stained with propidium iodide before analysis of DNA content via flow cytometry.

(A) Distribution of nuclei passed on DNA content for each genotype as indicated. Confidence interval of the proportion of each type of nuclei showing significant difference ($P<0.05$, t-test) is shown.

(B) 4c /2c nuclei ratio indicative of a first endocycle.

These nuclear DNA content analyses reveal no enhanced endoreduplication in petals of *bpe* or *arf8* single mutants. A slight increase in 2C content is observed in *bpe-1*. Conversely, a slight increase in 4C nuclei is observed in petals of the *bpe arf8* double mutant compared to the wild type. This increased ploidy is however not confirmed with additional endocycle.

Supplemental Table 1 : Sequence of primers used in this study

Primer	Gene	Sequence	Experiment
At SAUR r	<i>SAUR-AC1</i>	TATTGTTAACGCCGCCATTG	qRT-PCR
At SAUR l	<i>SAUR-AC1</i>	AAGGGAATCATCGTCGACAC	qRT-PCR
At IAA 1 R	<i>Aux/IAA1</i>	TGGACGGAGCTCCATATCTC	qRT-PCR
At IAA 1 F	<i>Aux/IAA1</i>	ACCGACCAACATCCAATCTC	qRT-PCR
At IAA 3 R	<i>Aux/IAA3</i>	TGATTGGATGCTATTGGTG	qRT-PCR
At IAA 3 F	<i>Aux/IAA3</i>	CAACCCAAGCACAGACAGAG	qRT-PCR
At IAA 9 R	<i>Aux/IAA9</i>	GAGCTGCTGGAAAGGATATG	qRT-PCR
At IAA 9 F	<i>Aux/IAA9</i>	GCTGCAGCTAACCAATAGC	qRT-PCR
At IAA 17 R	<i>Aux/IAA17</i>	AGGGTTCTCAGAGACGGTTG	qRT-PCR
At IAA 17 F	<i>Aux/IAA17</i>	TTGATTTTGGCAGGAAACC	qRT-PCR
At IAA 19 F2	<i>Aux/IAA19</i>	GACTCGGGCTTGAGATAACG	qRT-PCR
At IAA 19 R2	<i>Aux/IAA19</i>	CGTGGTCGAAGCTTCTTAC	qRT-PCR
ACT8 Q5	<i>ACT8</i>	GGTAACATTGTGCTCAGGGTG	qRT-PCR
ACT8 Q3	<i>ACT8</i>	AACGACCTTAATCTCATGCTG	qRT-PCR
TUB4 Q5	<i>TUB4</i>	AAGGCTTCTCTTATTGGTACA	qRT-PCR
TUB4 Q3	<i>TUB4</i>	CTCTCCGGCTGTAGCATCTT	qRT-PCR
TCTP-F	<i>TCTP</i>	CACCCAAGCTCAGCGAAGAA	qRT-PCR
TCTP-R	<i>TCTP</i>	CATGCATACCCCTCCCCAACAA	qRT-PCR
ARF8-5	<i>ARF8</i>	GACATGAAGCTGTCAACATCTGG	qRT-PCR
ARF8-m3	<i>ARF8</i>	TAGGTTGCTTACTCGGTATCC	qRT-PCR
BPEp-F	<i>BPEp</i>	CTGCTCCCCAAAACAGAACATT	qRT-PCR
BPEp-R	<i>BPEp</i>	TGCTTAGATGAACATAAGCGACTCCT	qRT-PCR
SD-D253-A-3	<i>BPEp</i>	CGAACCGCATAAACAGCGAGACTCTACCCCGAGA	Site directed mutagenesis Asp ²⁵³
SD-D253-A-5	<i>BPEp</i>	TCTCGGGGTAGGAGTCTCGCTGTTATCGGGTTCG	Site directed mutagenesis Asp ²⁵³
SD-F260-A-3	<i>BPEp</i>	CGTTTATTGCAATGCTTAGCTGACCGAACCGC	Site directed mutagenesis Phe ²⁶⁰
SD-F260-A-5	<i>BPEp</i>	CGGGTTGGTCAGCTAAGCATTGCAATAAACG	Site directed mutagenesis Phe ²⁶⁰
SD-R250-A-3	<i>BPEp</i>	GCATAAACATCGAGACTCGCACCCGAGAATAACCTCG	Site directed mutagenesis Arg ²⁵⁰
SD-R250-A-5	<i>BPEp</i>	CGAGGTTATTCTCGGGTGGCAGTCTCGATGTTATGC	Site directed mutagenesis Arg ²⁵⁰
BPEpORF-F	<i>BPEp</i>	GATTAAGTCCATGGATCCGAGTGGG	Cloning of <i>BPEp</i> ORF in pAS2.1
BPEpORF-R	<i>BPEp</i>	ATCCGCCGGGAATTCAAGAAAACAAAAACAGATTTTGA	
SDBPE-F	<i>BPEp</i>	CCGGAAATTGGGAAAGAGGGTGTGATTCTCATGATC	Cloning of SD ^{BPEp} in pAS2.1
BPEpORF-R	<i>BPEp</i>	ATCCGCCGGGAATTCAAGAAAACAAAAACAGATTTTGA	
ARF8CTD-F	<i>ARF8</i>	CACCCAAGACACAACATGAGT	Cloning of ARF8 in BiFC vector pBIFP3
ARF8CTD-R	<i>ARF8</i>	CTAGAGATGGTCGGGTTGC	
SDBPEBiFC-F	<i>BPEp</i>	GGGGACAAGTTGTACAAAAAAGCAGGCTAGGGTA	Cloning of <i>BPEp</i> in BiFC vector pBIFP2
SDBPEBiFC-R	<i>BPEp</i>	ATGATTCTCATGATCATC	
SDBPEBiFC-R	<i>BPEp</i>	GGGGACCACTTGTACAAGAAAGCTGGGTATCAAGAA	BPEp-GFP fusion Cloning
BPEpGFP-F	<i>BPEp</i>	AACAAAACAGATT	
BPEpGFP-R	<i>BPEp</i>	GGGGACCAACTTGTACAAGAAAGCTGGGTATCAAGAA	mOrange-ARF8 fusion Cloning
ARF8mOrang-F	<i>ARF8</i>	AACAAAACAGATT	
ARF8mOrang-R	<i>ARF8</i>	GGGGACCAACTTGTACAAGAAAGCTGGGTATCAAGAA	Mutagenesis of splice donor site for <i>BPEp</i> intron V
BPEpSplicMut-F	<i>BPEp</i>	GGGGACCAACTTGTACAAGAAAGCTGGGTATCAAGAA	
BPEpSplicMut-R	<i>BPEp</i>	GGGGACCAACTTGTACAAGAAAGCTGGGTATCAAGAA	